The endoplasmic reticulum-associated mRNA-binding proteins ERBP1 and ERBP2 interact in bloodstream-form *Trypanosoma brucei*.

Kathrin Bajak[a,b], Kevin Leiss[a], Christine Clayton[a] and *Esteban Erben[b]

[a]Heidelberg University Centre for Molecular Biology (ZMBH), Im Neuenheimer Feld 282, D69120 Heidelberg. Germany.
[b]Division of Immune Diversity, Deutsche Krebsforschungszentrum (DKFZ), Im Neuenheimer Feld 280, D69120 Heidelberg. Germany.

* Corresponding author: e.erben@dkfz-heidelberg.de

Abstract

Kinetoplastids rely heavily on post-transcriptional mechanisms for control of gene expression, and on RNA-binding proteins that regulate mRNA splicing, translation and decay. *Trypanosoma brucei* ERBP1 (Tb927.10.14150) and ERBP2 (Tb927.9.9550) were previously identified as mRNA binding proteins that lack canonical RNA-binding domains. We here show that ERBP1 is associated with the endoplasmic reticulum, like ERBP2, and that the two proteins interact *in vivo*. Loss of ERBP1 from bloodstream-form *T. brucei* initially resulted in a growth defect but proliferation was restored after more prolonged cultivation. Results from a pull-down of tagged ERBP1 suggest that it preferentially binds to ribosomal protein mRNAs. The ERBP1 sequence resembles that of *Saccharomyces cerevisiae* Bfr1, which also localises to the endoplasmic reticulum and binds to ribosomal protein mRNAs. However, unlike Bfr1, ERBP1 does not bind to mRNAs encoding secreted proteins, and it is also not recruited to stress granules after starvation.

Introduction

In *Trypanosoma brucei*, most regulation of gene expression is post-transcriptional. Protein-coding genes are arranged in polycistronic transcription units, and mRNAs are excised by *trans* splicing and polyadenylation [1]. Levels of constitutively expressed proteins and mRNAs are strongly influenced by codon usage [2, 3], while regulation during development, over the cell cycle, and in response to environmental conditions is effected mainly by RNA-binding proteins. The latter often, but not always, bind sequences in 3'-untranslated regions (3'-UTRs) [1]. All mRNAs - whether or not they are subject to specific regulation - are expected to be bound by numerous different proteins, forming a "messenger ribonucleoprotein" (mRNP) assembly.

T. brucei grows in mammalian blood and tissue fluids, and in the digestive system of Tsetse flies. The developmental stages that are most accessible to laboratory study are the bloodstream form, which grows at 37°C in glucose-rich media and corresponds to the form that grows in mammals, and the procyclic form, which is grown at 27°C in proline-rich medium and multiplies in the Tsetse midgut. Purification of mRNPs from bloodstream forms revealed at least 155 proteins that reproducibly could be cross-linked to, and co-purified with, mRNA [4]. Although many of the mRNA-binding proteins had recognizable consensus RNA-binding motifs, the list included 49 proteins, including that encoded by Tb927.10.14150, that had no obvious connection to RNA metabolism. Similar studies of Opisthokonts also revealed numerous novel proteins without known RNA-binding domains, which have been

named "enigmRBPs" [5, 6]. We will therefore call the Tb927.10.14150 protein ERBP1 (for EnigmRBP1).

To assess the ability of trypanosome proteins to affect mRNA stability or translation, they were "tethered" to a reporter RNA. To do this, proteins or protein fragments were expressed fused to the N peptide from bacteriophage lambda. The lambdaN peptide binds an RNA stem-loop called boxB with high affinity. The reporter mRNA encoded a selectable marker with boxB sequences in the 3'-UTR. Proteins were screened first as random fragments [7], then at full length [4]. Numerous regulators were found, many of which were also in the mRNP proteome [4], and ERBP1 reproducibly conferred a selective advantage when tethered both as fragments and at full length [4, 7]. ERBP1 fused C-terminally to GFP was associated with the endoplasmic reticulum in a high-throughput screen of procyclic forms [8] and its depletion resulted in a selective disadvantage in a high throughput RNAi screen [9].

In this paper we describe more detailed studies of ERBP1. ERBP1 is predicted to belong to a protein family that is named after a *S. cerevisiae* protein called Bfr1p (IPR039604 or PTHR31027), with alignment over its entire length. Bfr1p was originally recovered in a screen for high-copy-number suppression of Brefeldin A toxicity [10]. It is an mRNA-binding protein that is associated with polysomes and the endoplasmic reticulum (ER) [11, 12], and is incorporated into stress granules [13]. In yeast, it is associated with over 1000 different mRNAs, enriched for those encoding ribosomal proteins and mRNAs that are translated at the ER [14]. In addition to a role in stress granules, Bfr1 has been implicated in ER quality control [15] and correct nuclear segregation [16]. The physical interaction map (https://www.yeastgenome.org/locus/S000005724/interaction) includes five proteins related to mRNA decay: with Xrn1p, Dcp2p, Scp160p, Puf3p, and Asc1p (an orthologue of RACK1 that inhibits translation). Our results reveal that ERBP1 has both similarities with, and differences from, Bfr1.

Results

ERBP1 is conserved in *Trypanosoma*

To investigate the function of ERBP1, we first analysed its sequence. ERBP1 is a 55kDa protein with an isolelectric point of 5.73. It is predicted (by Phyre2) to consist predominantly of alpha-helices. Homologues are found at the equivalent chromosomal position in other *Trypanosoma* species, and in *Endotrypanum*, *Paratrypanosoma*, *Blechomonas* and *Bodo*, but the gene appears to have been lost in *Leishmania*. The alignment (Supplementary Fig S1) shows that the proteins share extremely acidic C-termini: for example, in *T. brucei*, the last 33 amino acid residues include 5 aspartates and 14 glutamates, as opposed to 3 lysines. Outside the Kinetoplastida, the nearest matches were not with yeast Bfr1p, but with proteins of unknown function in *Galdieria sulphuraria*, an acidiphilic red alga, and organisms from the SAR group that probably have incorporated red algal endosymbionts: the oomycete *Phytophthora parasitica*, the brown alga *Ectocarpus siliculosus* and the diatom *Phaeodactylum tricornutum*. The alignment with all these proteins, as well as Bfr1p, showed little sequence identity between the kinetoplastid sequences and all the others (S1 Fig).

ERBP1 is required for normal growth but is not essential

We first confirmed that ERBP1 is indeed required for normal growth of bloodstream-form trypanosomes. To do this, we created bloodstream forms in which one *ERBP1* gene was modified to encode a protein with an N-terminal V5 tag (V5-ERBP1). These were transfected

with a tetracycline-inducible construct for production of *ERBP1* dsRNA. Depletion of ERBP1 clearly inhibited cell proliferation but the cells nevertheless survived (Fig 1).

Since some protein always remains after RNAi, we also tested the ability of the cells to survive in the absence of the protein. Trypanosomes without ERBP1 (Fig 2A, B) also grew slower than wild-type (Fig 2C), and this could be compensated by re-expression of the protein (Fig 2D). Cells containing only a single tetracycline-inducible copy of ERBP1-myc (inducible on a knock-out background) grew at similar rates to wild-type with or without tetracycline, but the protein was clearly detectable in the absence of induction. Since tetracycline-inducible expression is effected from a very active RNA polymerase I promoter, the result suggests that excess ERBP1-myc is not toxic. Despite these initial results, upon prolonged cultivation, the cells lacking ERBP1 gradually increased their growth rate to wild-type. Survival and recovery of the cells after starvation was also indistinguishable from wild-type (S2 Fig A). In procyclic forms, the endogenous ERBP1 gene could be deleted only if an inducible ERBP1-myc gene was present. Depletion of the ERBP1-myc had no effect on growth or recovery from starvation (S2 Fig B), but some residual ERBP1-myc was doubtless present. It is therefore possible that ERBP1 is essential in procyclic forms, but the failure of the deletion could also have been due to a technical problem.

The other high-throughput result that required verification was the effect of ERBP1 when tethered to a reporter mRNA. Full-length ERBP1 had previously been identified as conferring a selective advantage in the screen, suggesting that it could activate expression of the blasticidin resistance marker. It gave no growth advantage in control cells in which when the marker mRNA had no boxB sequences, ruling out the possibility that ERBP1 expression by itself results in blasticidin resistance. However, lambdaN-ERBP1 was unable to increase expression of a chloramphenicol acetyltransferase reporter (S3 Fig). We have no explanation of this discrepancy: for both the screen and the individual test, the lambdaN-myc sequence was placed at the N-terminus of the open reading frame.

ERBP1 is associated with the endoplasmic reticulum and with a second ER protein

To examine the location of ERBP1 we examined either N-terminally V5-tagged ERBP1 (V5-ERBP1), or C-terminally myc-tagged ERBP1 (ERBP1-myc) expressed from the endogenous locus (Figure 3). In both cases, ERBP1 clearly co-localized with the endoplasmic reticulum (Figure 4). After digitonin fractionation, ERBP1 behaved like a cytosolic protein (Figure 5), suggesting that it is loosely associated with the cytosolic face of the ER.

To investigate the interactions of ERB1, we used trypanosomes in which ERBP1 a sequence encoding a tandem affinity purification (TAP) tag was integrated at the N-terminus, and the other copy of *ERBP1* was deleted. TAP-tagged GFP served as the control. Three proteins reproducibly co-purified with ERBP1: calmodulin, the DED1-like helicase Tb927.10.14550, and a protein of unknown function encoded by Tb927.9.9550 (S1 Table). Calmodulin quite often co-purifies with tagged proteins. The association with the DED1 helicase may be significant, although we have identified on most other mRNA-related purifications. Tb927.9.9550, however, was a novel protein partner. It is conserved throughout Kinetoplastida, activated in the tethering screen, is in the mRNP proteome, but again lacks any recognisable domains; we therefore call it ERBP2. It appeared to be essential in the high-throughput RNAi screen [9], has a predicted signal peptide and trans-membrane domain, and a GFP-tagged version, like ERBP1, localised to the ER [8]. To verify the interaction we used cells containing YFP-in-situ tagged ERBP1, with or without expression of ERBP2-myc. YFP-ERBP1 was pulled down with anti-myc antiserum only if ERBP2-myc was present, confirming the interaction (Figure 6A), but the experiment also showed that - at least

under the conditons used - only a very small proportion of the ERBP1 was associated with ERBP2. This may, therefore, be a transient interaction. ERBP2 is predicted to be predominantly alpha-helical, like ERBP1. The isoelectric point of ERBP2 is 11, so it might interact with the highly acidic ERBP1 C-terminus.

ERBP1 associates with mRNAs encoding ribosomal proteins, and not with starvation stress granules

Finally, we wished to know whether ERBP1 had any mRNA-binding specificity. We therefore sequenced mRNAs that were co-purified with TAP-ERBP1, comparing them either with one unbound fraction or with the total mRNA. Unusually, the *ERBP1* mRNA itself was not enriched, as would be expected from pull-down of the nascent polypeptide. However, the two bound fractions clearly separated from all the controls (Figure 6B). 64 mRNAs were enriched at least 2-fold in both pull-downs relative to all controls. Strikingly, nearly half of them (29) encode ribosomal proteins. Two glycosomal membrane protein mRNAs, PMP4 and PEX11, were also enriched, but those encoding other PEX proteins - including other glycosomal membrane proteins - were not, so the significance of this is uncertain.

It should be noted that the enrichment of mRNAs is calculated relative to the enrichment of other mRNAs, and does not actually tell us which proportion of mRNAs with that sequence is associated with the protein *in vivo*.

Brf1 is associated with stress granules. To find out whether ERBP1 is stress-granule associated, we incubated procyclic forms in PBS for 2 hours. Although clear granules containing the marker SCD6 were formed (Figure 7A), V5-ERBP1 remained distributed throughout the cytosol (Figure 7A) and was not associated with the granule fraction (Figure 7B). There is therefore no evidence that ERBP1 is involved in formation of stress granules or survival after starvation.

Discussion

Our results suggest that ERBP1 and its partner ERBP2 may modulate ribosomal expression, and are both associated with the endoplasmic reticulum. Our results revealed both similarities and differences between ERBP1 and Bfr1. Each is associated with the endoplasmic reticulum, and each binds preferentially to mRNAs encoding ribosomal proteins. ERBP1, however, unlike Bfr1, does not show any preference for mRNAs encoding proteins that are imported into the endoplasmic reticulum, and it does not associate with stress granules. The latter observation is consistent with the exclusion of ribosomal protein mRNAs from trypanosome stress granules. ERBP1 is also associated with a kinetoplastid-specific protein, ERBP2 which, like ERBP1, was detected in the mRNP proteome.

Synthesis of ribosomes occupies considerable resources in all growing cells, which leads to a requirement for coordination between ribosomal protein synthesis and rRNA transcription. In mammalian cells and yeast, this coordination happens in the nucleus, at the level of transcription [17, 18]. Trypanosomes also devote considerable resources to ribosome synthesis: in bloodstream-forms, resources devoted to rRNA transcription are at least as great as those needed for synthesis of mRNAs [19], and the ribosomal protein mRNAs together constitute more than 10% of total mRNA [20]. Feedback inhibition of rRNA processing is known to occur in trypanosomes upon disruption of ribosome assembly or export [21], but coordination of rRNA sythesis with ribosomal protein availability - or vice-versa - has not been investigated. The mRNAs encoding trypanosome ribosomal proteins are longer-lived than most others [20], so at least in the short term, control of their translation

might be required in order to respond to altered conditions. Ribosome densities on ribosomal protein mRNAs are significantly lower than on other mRNAs, and most of the open reading frames are also relatively short (median 0.6kb); consequently on average there is only one ribosome per mRNA [22]. Low ribosome densities occur if the rate of peptide chain elongation is fast relative to the rate of translation initiation. Ribosomal protein mRNAs indeed have optimal codon usage [2], which would result in rapid elongation, and their short 5'-untranslated regions [1] might assist scanning after 43S complex recruitment. These characteristics would lead to constitutive high expression, but would also enable very rapid responses to altered conditions since, at 5-10 residues per second, the single ribosome would run off in less than 1 minute. We therefore suggest that several redundant pathways control ribosome protein synthesis, and one of them includes ERBP1.

Materials and Methods

DNA manipulation and trypanosomes

Lister 427 strain trypanosomes expressing the tet repressor were used for all experiments, and were cultivated and transfected as described previously [23]. All plasmids and oligonucleotides are listed in S3 Table. Expression from tetracycline-inducible promoters was induced with 100ng/ml tetracycline, and all growth studies were performed in the absence of selecting antibiotics. Cultures that were used for RNA and protein analysis had a maximum density of $1.5x10^6$/ml.

Western blotting

$3\text{-}5x10^6$ cells were collected per sample, resuspended in 6x Laemmli Buffer and heated at 95°C for 10 min. The samples were subjected to SDS-PAGE gel electrophoresis using 10% polyacrylamide gels. The gels were then stained with SERVA blue G or blotted on a 0.45 µm nitrocellulose blotting membrane (Neolabs). To verify the protein transfer, the membrane was stained with Ponceau S (SERVA). The membrane was blocked with 5% milk in TBS-Tween and incubated with appropriate concentrations of first and secondary antibodies. Western Lightning Ultra (Perkin Elmer) was used as chemiluminescence system and signals were detected with the LAS-4000 imager (GE Healthcare) and CCD camera (Fujifilm). Antibodies used were: rabbit anti-aldolase (1:50000) [24]; mouse anti-myc 9E10 (Santa Cruz, 1:200); rabbit Peroxidase ant-peroxidase (Sigma, 1:20000); rat anti-ribosomal protein S9 (1:1000); anti-trypanothione reductase (rabbit, gift from Luise Krauth-Siegel, BZH Heidelberg); Mouse anti-V5 (Biorad, 1:2000); Anti-SCD6 and anti-DHH1 (From Susanne Kramer, 1:10000 and 1:15000 respectively) and rabbit anti-BiP(from J. Bangs, University of Buffalo, 1:1000).

Digitonin and stress granule fractionation

For each sample $3x10^7$ cells were collected by centrifugation at 2000g for 10 min at 4°C. The pellet was resuspended in 100 µl 1x PBS and centrifuged at 10000g for 5 min at 4°C. Pellet was resuspended in 50 µl STE buffer (10mM Tris-Cl pH 8, 150 mM NaCl, 1mM EDTA)) and centrifuged at 10000g for 5 min at 4°C. A 10 µg/µl digitonin stock solution was heated at 98°C for 5 min and cooled down before use. Seven different digitonin containing solutions, ranging from 0-1.65 µg/µl digitonin, were prepared and each pellet was resuspended properly in 60 µl of one solution. The samples were incubated at 25°C for 5 min and then centrifuged immediately at 10000g and 4°C for 5min. The supernatant was transferred to another tube containing 20 µl 4x SDS-PAGE sample buffer. The pellet was washed twice

with 1x PBS by centrifugation (4°C, 10000g, 5 min) and finally resuspend it in 80 µl 1x Laemmli buffer. Samples were analyzed by Western Blotting.
Stress granules were purified exactly as described in [25], and immunoprecipitations were done as described in [26].

Immunofluorescence microscopy

Tissue culture glass slides with 8 chambers were treated with 0.1% Poly-Lysine (Sigma, P-8920). $2.5x10^6$ formaldehyde-fixed *T. brucei* were allowed to adhere to poly-lysine-treated chambered slides (Falcon, 354108), permeabilised with 0.2% (w/v) Triton X-100 then incubated with protein-specific antibodies followed fluorescently-labelled second antibodies in PBS containing 0.5% gelatin. DNA was stained with 100 ng/ml DAPI (D9542, Sigma-Aldrich). MItochondria were detected by addition of Mitotracker Red CMXRos (50 nM, Thermo Fisher Scientific) to the cells 5 min prior to fixation. Images were examined using the Olympus IX81 microscope, 100x Oil objective with a numerical aperture of 1.45. Digital images were taken with ORCA-R2 digital CCD camera C10600 (Hamamatsu) and using the Xcellence rt software. The bright field images were taken using differential interference contrast (DIC). Fluorescent images were taken as Z-Stacks with a high of roughly 4 µm and a step width of 0.2 µm. The images were deconvoluted (Wiener Filter, Sub-Volume overlap: 20) and then processed using ImageJ. The background was subtracted and brightness and contrast were adjusted automatically. The most in focus image of the deconvoluted stack was used.

RNA preparation and Northern blotting

$5x10^7$ cells were used for the extraction of total mRNA using peqGold Trifast (peqLab). RNA was separated on Agarose-Formaldehyde gels and blotted on a nylon membrane (Amersham Hybond-N+, GE Healthcare, RPN203B). RNA was cross-linked on membrane by UV light (2x240 mJoules) and stained afterwards with methylene blue (SERVA) before hybridisation with ^{32}P-labelled probes, made using either the Prime-IT RmT Random Primer Labelling Kit (Stratagene) or, for oligonucleotides, [γ^{32}P]ATP and T4 polynucleotide kinase (New England Biolabs).

Affinity purification and mass spectrometry

To purify TAP-ERBP1 for mass spectrometry, the protein was subjected to two steps of affinity purification [27]. Briefly, the cleared lysate was incubated with IgG sepharose beads, washed, and then bound proteins were released using TEV protease. The resulting preparation was then allowed to adhere to a calmodulin affinity column, and proteins were eluted with EGTA. Co-purifying proteins from three independent experiments were anlysed by LC/MS by the ZMBH Mass Spectrometry facility. Cell lines expressing TAP-GFP served as control. Raw data were analyzed using MaxQuant 1.5.8.3, with label-free quantification (LFQ), match between runs (between triplicates), and the iBAQ algorithm enabled. The identified proteins were filtered for known contaminants and reverse hits, as well as hits without unique peptides.

Affinity purification and RNASeq

For identification of associated RNAs [28], 1 $x10^9$ cells the cells were resuspended in 50 ml ice-cold PBS, and UV-crosslinked (2x2400 µJoules, Stratagene UV crosslinker) in two P15 Petri dishes on ice. They were then pelletted, snap-frozen and stored in liquid nitrogen before use. The TAP-ERBP1 was allowed to bind to IgG beads, and unbound lysate was retained as one of the controls. The bound protein was released using TEV protease. Cross-linked

proteins were removed by proteinase K digestion [28] and RNA was extracted using peqGold Trifast (peqLab) according to manufacturer's protocol. rRNA was depleted as required, by incubation with complementary oligonucleotides and RNaseH [29]. The NEBNext Ultra RNA Library Prep Kit for Illumina (New England BioLab) was used for library preparation, prior to sequencing with sequenced at EMBL (HiSeq 2000) to generate 50-base reads. Data was analysed using an in-house tool (10.5281/zenodo.165132) [30].

Acknowledgements

We thank Nina Papavisiliou for generously hosting KB during the latter part of this project. We also acknowledge Claudia Helbig and Ute Leibfried for technical support, David Ibberson of the BioQuant sequencing facility for cDNA library construction, and the Mass spectrometry facility of the ZMBH. We thank Luise Krauth-Siegel, (BZH Heidelberg), Susanne Kramer (University of Würzberg) and Jay Bangs (University of Buffalo) for antibodies, and Pia Hartwig for work done during a lab rotation. This project was partially supported by the Deutsche Forschungsgemeinshaft (grant CI112/24 to CC).

References

1. Clayton C. Control of gene expression in trypanosomatids: living with polycistronic transcription. Royal Society Open BIology. 2019;9:190072. doi: 10.1098/rsob.190072.
2. de Freitas Nascimento J, Kelly S, Sunter J, Carrington M. Codon choice directs constitutive mRNA levels in trypanosomes. eLife. 2018;7. Epub 2018/03/16. doi: 10.7554/eLife.32467. PubMed PMID: 29543152; PubMed Central PMCID: PMCPMC5896880.
3. Jeacock L, Faria J, Horn D. Codon usage bias controls mRNA and protein abundance in trypanosomatids. eLife. 2018;7. Epub 2018/03/16. doi: 10.7554/eLife.32496. PubMed PMID: 29543155; PubMed Central PMCID: PMCPMC5896881.
4. Lueong S, Merce C, Fischer B, Hoheisel J, Erben E. Gene expression regulatory networks in *Trypanosoma brucei*: insights into the role of the mRNA-binding proteome. Molecular microbiology. 2016;100:457-71. PubMed Central PMCID: PMCdoi: 10.1111/mmi.13328 PMID: 26784394.
5. Hentze MW, Castello A, Schwarzl T, Preiss T. A brave new world of RNA-binding proteins. Nat Rev Mol Cell Biol. 2018. Epub 2018/01/18. doi: 10.1038/nrm.2017.130. PubMed PMID: 29339797.
6. Beckmann BM, Horos R, Fischer B, Castello A, Eichelbaum K, Alleaume AM, et al. The RNA-binding proteomes from yeast to man harbour conserved enigmRBPs. Nat Commun. 2015;6:10127. PubMed Central PMCID: PMC10.1038/ncomms10127
Pmc4686815.
7. Erben E, Fadda A, Lueong S, Hoheisel J, Clayton C. Genome-wide discovery of post-transcriptional regulators in *Trypanosoma brucei*. PLoS pathogens. 2014;10:e1004178. doi: doi:10.1371/journal.ppat.1004178. PubMed Central PMCID: PMCdoi:10.1371/journal.ppat.1004178.
8. Dean S, Sunter J, Wheeler R. TrypTag.org: A trypanosome genome-wide protein localisation resource. Trends Parasitol. 2016;33:80-2.
9. Alsford S, Glover L, Horn D. Multiplex analysis of RNA interference defects in Trypanosoma brucei. Molecular and biochemical parasitology. 2005;139(1):129-32. PubMed PMID: 15610827.
10. Jackson CL, Kepes F. BFR1, a multicopy suppressor of brefeldin A-induced lethality, is implicated in secretion and nuclear segregation in Saccharomyces cerevisiae. Genetics. 1994;137(2):423-37. Epub 1994/06/01. PubMed PMID: 8070655; PubMed Central PMCID: PMCPMC1205967.
11. Lang BD, Li A, Black-Brewster HD, Fridovich-Keil JL. The brefeldin A resistance protein Bfr1p is a component of polyribosome-associated mRNP complexes in yeast. Nucleic acids research. 2001;29(12):2567-74. Epub 2001/06/19. doi: 10.1093/nar/29.12.2567. PubMed PMID: 11410665; PubMed Central PMCID: PMCPMC55738.
12. Weidner J, Wang C, Prescianotto-Baschong C, Estrada AF, Spang A. The polysome-associated proteins Scp160 and Bfr1 prevent P body formation under normal growth conditions. J Cell Sci. 2014;127(Pt 9):1992-2004. Epub 2014/02/27. doi: 10.1242/jcs.142083. PubMed PMID: 24569876.
13. Simpson CE, Lui J, Kershaw CJ, Sims PF, Ashe MP. mRNA localization to P-bodies in yeast is bi-phasic with many mRNAs captured in a late Bfr1p-dependent wave. J Cell Sci. 2014;127(Pt

6):1254-62. Epub 2014/01/16. doi: 10.1242/jcs.139055. PubMed PMID: 24424022; PubMed Central PMCID: PMCPMC3953815.
14. Lapointe CP, Wilinski D, Saunders HA, Wickens M. Protein-RNA networks revealed through covalent RNA marks. Nat Methods. 2015;12(12):1163-70. Epub 2015/11/03. doi: 10.1038/nmeth.3651. PubMed PMID: 26524240; PubMed Central PMCID: PMCPMC4707952.
15. Low YS, Bircham PW, Maass DR, Atkinson PH. Kinetochore genes are required to fully activate secretory pathway expansion in S. cerevisiae under induced ER stress. Mol Biosyst. 2014;10(7):1790-802. Epub 2014/04/12. doi: 10.1039/c3mb70414a. PubMed PMID: 24722431.
16. Xue Z, Shan X, Sinelnikov A, Melese T. Yeast mutants that produce a novel type of ascus containing asci instead of spores. Genetics. 1996;144(3):979-89. Epub 1996/11/01. PubMed PMID: 8913743; PubMed Central PMCID: PMCPMC1207637.
17. Albert B, Knight B, Merwin J, Martin V, Ottoz D, Gloor Y, et al. A Molecular Titration System Coordinates Ribosomal Protein Gene Transcription with Ribosomal RNA Synthesis. Molecular cell. 2016;64(4):720-33. Epub 2016/11/08. doi: 10.1016/j.molcel.2016.10.003. PubMed PMID: 27818142.
18. Calo E, Flynn RA, Martin L, Spitale RC, Chang HY, Wysocka J. RNA helicase DDX21 coordinates transcription and ribosomal RNA processing. Nature. 2015;518(7538):249-53. Epub 2014/12/04. doi: 10.1038/nature13923. PubMed PMID: 25470060; PubMed Central PMCID: PMCPMC4827702.
19. Haanstra J, Stewart M, Luu V-D, van Tuijl A, Westerhoff H, Clayton C, et al. Control and regulation of gene expression: quantitative analysis of the expression of phosphoglycerate kinase in bloodstream form *Trypanosoma brucei*. J Biol Chem. 2008;283:2495-507.
20. Fadda A, Ryten M, Droll D, Rojas F, Färber V, Haanstra J, et al. Transcriptome-wide analysis of mRNA decay reveals complex degradation kinetics and suggests a role for co-transcriptional degradation in determining mRNA levels. Molecular microbiology. 2014;94:307-26. doi: 10.1111/mmi.12764. PubMed Central PMCID: PMCdoi: .
21. Droll D, Archer S, Fenn K, Delhi P, Matthews K, Clayton C. The trypanosome Pumilio-domain protein PUF7 associates with a nuclear cyclophilin and is involved in ribosomal RNA maturation. FEBS Lett. 2010;84:1156-62. doi: 10.1016/j.febslet.2010.02.018.
22. Antwi E, Haanstra J, Ramasamy G, Jensen B, Droll D, Rojas F, et al. Integrative analysis of the *Trypanosoma brucei* gene expression cascade predicts differential regulation of mRNA processing and unusual control of ribosomal protein expression. BMC genomics. 2016;17:306. doi: 10.1186/s12864-016-2624-3.
23. Alibu VP, Storm L, Haile S, Clayton C, Horn D. A doubly inducible system for RNA interference and rapid RNAi plasmid construction in *Trypanosoma brucei*. Mol Biochem Parasitol. 2004;139:75-82.
24. Clayton CE. Import of fructose bisphosphate aldolase into the glycosomes of *Trypanosoma brucei*. J Cell Biol. 1987;105:2649-53.
25. Fritz M, Vanselow J, Sauer N, Lamer S, Goos C, Siegel T, et al. Novel insights into RNP granules by employing the trypanosome's microtubule skeleton as a molecular sieve. Nucleic Acids Res 2015;43:8013-32. PubMed Central PMCID: PMCdoi:10.1093/nar/gkv731.
26. Singh A, Minia I, Droll D, Fadda A, Clayton C, Erben E. Trypanosome MKT1 and the RNA-binding protein ZC3H11: interactions and potential roles in post-transcriptional regulatory networks. Nucleic acids research. 2014;42:4652-68. doi: 10.1093/nar/gkt1416. PubMed Central PMCID: PMCPMC3985637.
27. Estévez AM, Lehner B, Sanderson CM, Ruppert T, Clayton C. The roles of inter-subunit interactions in exosome stability. J Biol Chem. 2003;278:34943-51.
28. Droll D, Minia I, Fadda A, Singh A, Stewart M, Queiroz R, et al. Post-transcriptional regulation of the trypanosome heat shock response by a zinc finger protein. PLoS pathogens. 2013;9:e1003286. PubMed Central PMCID: PMC10.1371/journal.ppat.1003286.
29. Minia I, Merce C, Terrao M, Clayton C. Translation regulation and RNA granule formation after heat shock of procyclic form *Trypanosoma brucei*: many heat-induced mRNAs are increased during differentiation to mammalian-infective forms. PLoS neglected tropical diseases. 2016;10:e0004982. PubMed Central PMCID: PMC10.1371/journal.pntd.0004982.
30. Mulindwa J, Leiss K, Ibberson D, Kamanyi Marucha K, Helbig C, Melo do Nascimento L, et al. Transcriptomes of *Trypanosoma brucei rhodesiense* from sleeping sickness patients, rodents and culture: Effects of strain, growth conditions and RNA preparation methods. PLoS neglected tropical diseases. 2018;12(2):e0006280. Epub 2018/02/24. doi: 10.1371/journal.pntd.0006280. PubMed PMID: 29474390; PubMed Central PMCID: PMCPMC5842037.
31. Moretti NS, Cestari I, Anupama A, Stuart K, Schenkman S. Comparative Proteomic Analysis of Lysine Acetylation in Trypanosomes. Journal of proteome research. 2018;17(1):374-85. Epub 2017/11/24. doi: 10.1021/acs.jproteome.7b00603. PubMed PMID: 29168382.

32. Urbaniak MD, Martin D, Ferguson MA. Global quantitative SILAC phosphoproteomics reveals differential phosphorylation is widespread between the procyclic and bloodstream form lifecycle stages of *Trypanosoma brucei*. Journal of proteome research. 2013;12:2233-44. Epub 2013/03/15. doi: 10.1021/pr400086y. PubMed PMID: 23485197.

Figure Legends

Figure 1:
ERBP1 is required for normal growth of bloodstream-form *T. brucei*

Bloodstream forms in which one *ERBP1* gene was V5-tagged in situ at the 5'-end were used, with inducible expression of stem-loop *ERBP1* dsRNA.

A. Depletion of V5-ERBP1 after RNAi. $3x10^6$ cells were collected each day and V5-ERBP1 was detected by Western Blotting. Aldolase was used as loading control.

B. Growth curve for three clones analysed in three independent experiments. Error bars indicate standard deviation for all nine sets of values. Tet+ (red) and Tet- (grey). Division times (in h) for the 3 experiments are on the right.

Figure 2
Bloodstream-form trypanosomes survive without ERBP1

A. Schematic representation of the *ERBP1* gene before and after replacement with selectable marker genes. Primers for PCR and corresponding product lengths (in kb) are shown.

B. DNA from wild type (WT) and *ERBP1*$^{-/-}$ (HKO) cells was analysed by PCR using the primers shown in (A). The primers used are indicated above each image.

C. Cumulative growth curves for 3 independent clones, for wild-type (WT), SKO and *erbp1* HKO.

D. Expression of ERBP1-myc complements the defect in *erbp1*$^{-/-}$ cells. The HKO was complemented with tetracycline-inducible ERBP1-myc. The upper panel shows cumulative parasite numbers and the lower panel is a Western blot from ($3x10^6$ cells/lane). Some ERBP1-myc is detectable in the absence of tetracycline inducer. The double band from ERBP1 was not always seen but might be caused by acetylation [31] or phosphorylation [32].

E. As (D) but for procyclic forms. Aldolase was used as loading control. Homozygous gene replacement failed in procyclic forms.

Figure 3
V5-ERBP1 colocalises with the endoplasmic reticulum.

Bloodstream forms expressing N-terminally V5-tagged ERBP from the endogenous locus (V5-ERBP1) were examined by immunofluorescence microscopy. Cells without V5 served as control. Nuclear and kinetoplast DNA was stained with DAPI (blue). Representative images are shown for three independent experiments. Z-stacks were examined using the Olympus CellR microscope and 100 x magnification, and Images were deconvoluted. Scale bar: 10 µm.

A. V5-ERBP1 is red and cytosolic Trypanothione Reductase (=TR) is green.

B. V5-ERBP1 is red and glycosomal aldolase is green.

C. V5-ERBP1 is green and mitotracker is red

D. V5-ERBP1 is red and the endoplasmic reticulum marker BiP is green.

Figure 4
ERBP1-myc colocalises with the endoplasmic reticulum.

Bloodstream forms expressing C-terminally myc-tagged ERBP from the endogenous locus (ERBP1-myc) were examined by immunofluorescence microscopy. Cells without myc served as control.

Nuclear and kinetoplast DNA was stained with DAPI (blue). Representative images rare shown for three independent experiments. Z-stacks were examined using the Olympus CellR microscope and 100 x magnification, and Images were deconvoluted. Scale bar: 10 µm.

A. ERBP1-myc is red and cytosolic Trypanothione Reductase (=TR) is green.

B. ERBP1-myc is red and glycosomal aldolase is green.

C. ERBP1-myc is green and mitotracker is red

D. ERBP1-myc is red and the endoplasmic reticulum marker BiP is green.

Figure 5
ERBP1 is not inside a membrane-bound compartment.

Bloodstream-form cells expressing V5-ERBP1 (**A**) or ERBP1-myc (**B**) were treated with increasing digitonin:protein (mg:mg) ratios as indicated at the top. Samples were centrifuged and the supernatant and pellet were analysed by Western Blotting. Numbers below the blots indicate quantification of the corresponding signal. TR: Trypanothione Reductase (cytosol); LipDH: Lipoamide Dehydrogenase (mitochondria); BiP: binding immunoglobulin protein (ER).

Figure 6:
Interactions of ERBP1

A. ERBP2 co-precipitates with ERBP1. Extracts were made from cells expressing YFP-ERBP1, with or without ERBP2-myc. After immunoprecipitation with anti-myc, a Western blot was probed for myc and for YFP as indicated. The stained membrane is shown below. I = input; UB = unbound fraction; E = eluate from anti-myc immunoprecipitation. The eluates are from 11 times more cells than were used for the input and unbound lanes.

B. Principal component analysis of transcriptomes after RNA-Seq of total mRNA (WT, wild-type cells) and after pull-down of TAP-ERBP1 - UB = unbound, B - bound (eluate from the affinity matrix).

C. Functions of proteins encoded by ERBP1-associated mRNAs. The pie chart show the distributions for mRNAs that were at least 2-fold enriched in both bound fractions relative to the controls. Details are in S2 Table.

Figure 7:
V5-ERBP1 is not concentrated in starvation stress granules

A. Procyclic forms expressing V5-ERBP1 were incubated for 2h in 1xPBS, then fixed and stained for V5 (red) and the stress granule marker SCD6 (green). Nuclear and kinetoplast DNA were stained with DAPI (blue). Z-stacks were examined using the Olympus CellR microscope and 100 x magnification. Images were deconvoluted. The control was not starved in PBS.

B. V5-ERBP1-expressing procyclic forms were starved as in (A) and then fractionated to concentrate stress granules as described in [25].

Supplementary Figures and Tables

Supplementary Figure S1
Alignment of ERBP1 homologues and BFR1.

The alignment was done using CLUSTAL. A key and the tree are on page 3.

Supplementary Figure S2
ERBP1 expression has no effect on survival after starvation.

A. Bloodstream-form cells were starved in PBS for 2h then returned to normal medium. Growth is on the left. The lines are: wild-type (WT), homozygous knock-out (HKO) and HKO trypanosomes complemented with tetracycline-inducible ERBP1-myc (cHKO) with (+) or without (-) tetracycline. A Western blot showing expression of ERBP1-myc is on the right.

B. As (A), except that procyclic forms were starved for 3h.

These experiments were done only once.

Supplementary Figure S3
ERBP1 did not activate of CAT expression when tethered.

A. Expression of chloramphenicol acetyltransferase (CAT) was measured in cells expressing different lambdaN-myc fusion proteins (ERBP1 and XAC1). XAC1 is Tb927.7.2780, which is a known activator of gene expression, served as control. Expression of the lambda-N proteins was induced with tetracycline (+Tet) for 24h. Results show arithmetic mean (black bar) & individual values of 3 independent experiments.

B. Expression of the myc-lambda-N-fusion proteins was validated by Western Blotting.

Supplementary Table S1
Quantitative mass spectrometry results for purification of TAP-ERBP1. TAP-GFP served as a control.

Supplementary Table S2
RNASeq results for purification of TAP-ERBP1.

Legend on the first sheet.

Supplementary Table S3
Plasmids and oligonucleotides

A

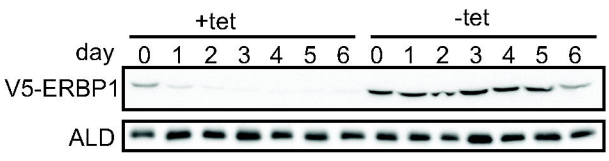

B

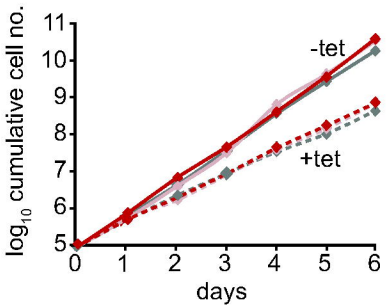

Division times (h)

	A	B	C
-tet	7.8	7.6	8.1
+tet	11.2	11.4	12.1

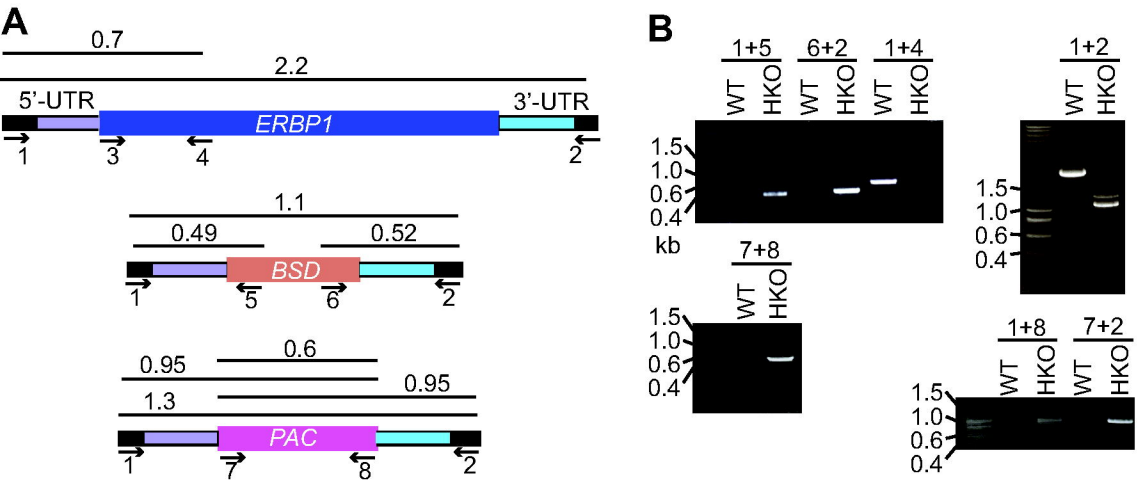

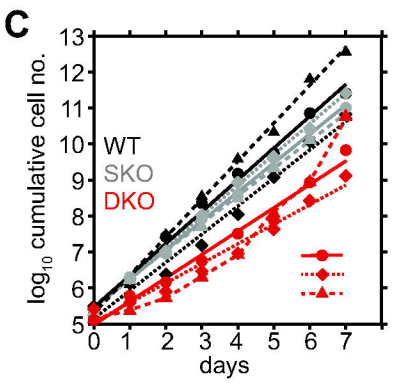

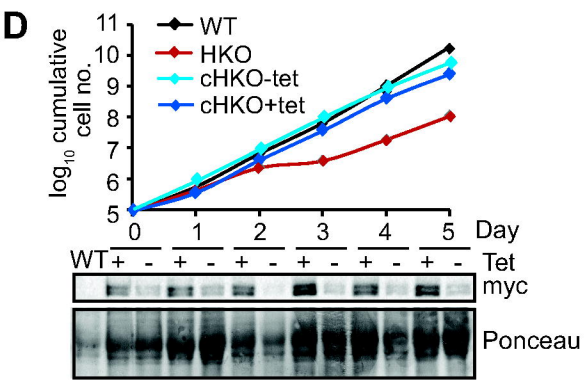

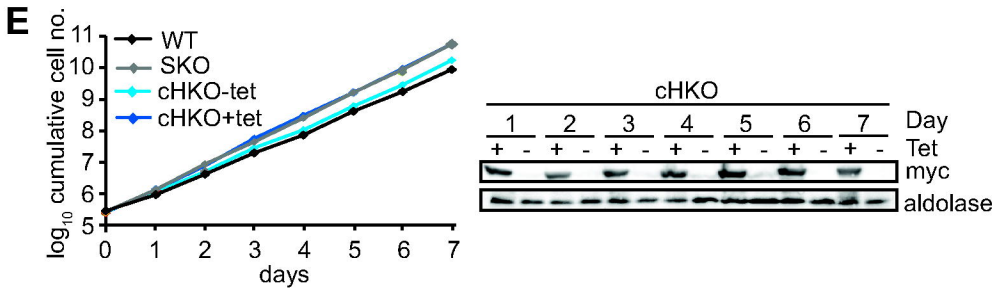

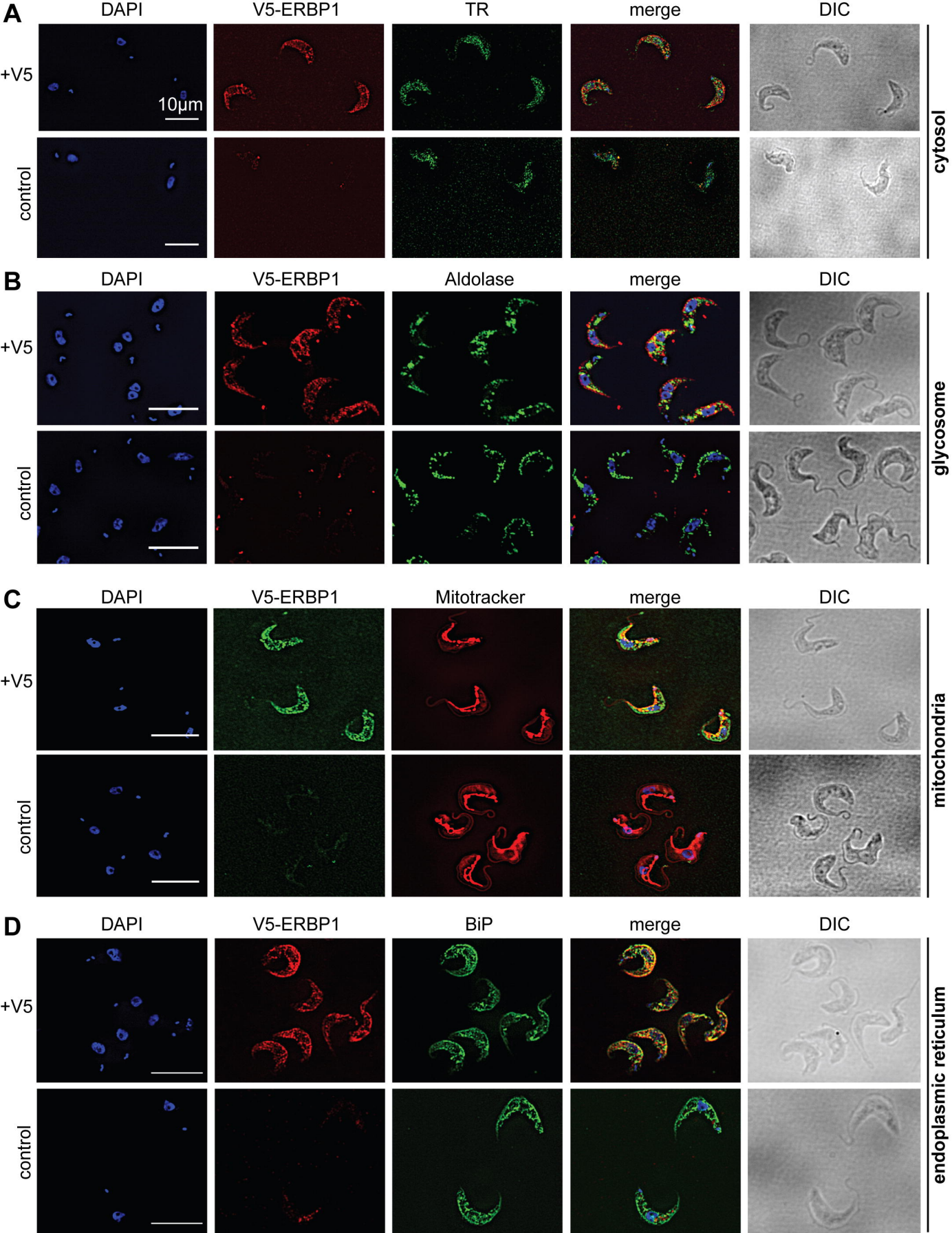
A
DAPI
V5-ERBP1
TR
merge
DIC
+V5
control
10μm
cytosol
B
DAPI
V5-ERBP1
Aldolase
merge
DIC
+V5
control
glycosome
C
DAPI
V5-ERBP1
Mitotracker
merge
DIC
+V5
control
mitochondria
D
DAPI
V5-ERBP1
BiP
merge
DIC
+V5
control
endoplasmic reticulum

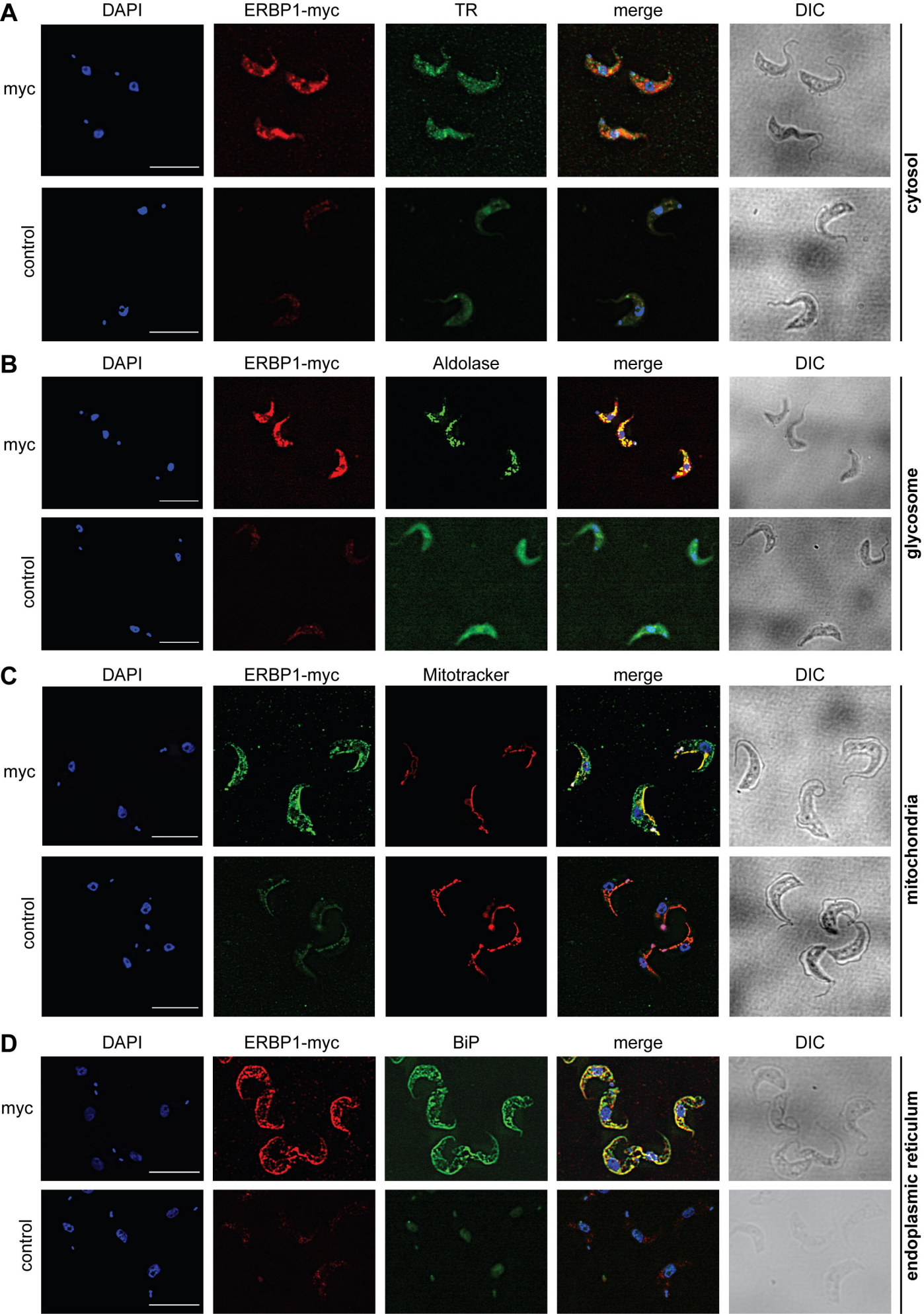
A
DAPI
ERBP1-myc
TR
merge
DIC
myc
control
cytosol
B
DAPI
ERBP1-myc
Aldolase
merge
DIC
myc
control
glycosome
C
DAPI
ERBP1-myc
Mitotracker
merge
DIC
myc
control
mitochondria
D
DAPI
ERBP1-myc
BiP
merge
DIC
myc
control
endoplasmic reticulum